J. Fluid Mech. (1985), *vol.* 154, *pp.* 1–28
Printed in Great Britain

Moving contact lines on a two-dimensional rough surface

By KALVIS M. JANSONS
Department of Applied Mathematics and Theoretical Physics, University of Cambridge, Silver Street, Cambridge CB3 9EW

(Received 24 July 1984)

The dynamic contact angle for a contact line moving over a solid surface with random sparse spots of roughness is determined theoretically in the limit of zero capillary number. The model exhibits many of the observed characteristics of moving contact lines on real rough surfaces, including contact-angle hysteresis and stick–slip. Several types of rough surface are considered, and a comparison is made between periodic and random rough surfaces.

1. Introduction

In this paper we study problems involving moving contact lines. A 'contact line' is the line of intersection of two immiscible fluids with a solid boundary. Two ingredients of such problems have received much attention in the past (Dussan V. 1979). The first is why the contact line is able to move given that classical fluid mechanics (i.e. that modelled by the Navier–Stokes equation, with a condition of no-slip at solid boundaries) forbids this possibility through a prediction of infinite stress at a moving contact line. The second concerns the dynamic contact angle, i.e. informally, the angle that a free surface makes with a solid surface at a moving contact line. It is always found experimentally (Dussan V. 1979) that the dynamic contact angle, considered as a function of the normal velocity of the contact line, is discontinuous at zero velocity. Many authors (including Huh & Mason 1977; Bayramli, van de Ven & Mason 1981; Cox 1983) have made steps towards explaining this phenomenon by considering surface roughness, although the rough surfaces considered have been far from realistic. All previous models of rough surfaces that have explained the discontinuity in the contact angle have either assumed that the surfaces are periodic (Huh & Mason 1977; Cox 1983), or one-dimensional and random (Bayramli *et al.* 1981). It will be shown in §3 that such surfaces exhibit many characteristics that are neither shared by two-dimensional random rough surfaces nor observed in practice.

Sections 2 and 3 of this work comprise a discussion of 'static' and 'dynamic' contact angles (though, as explained in §3, these terms are not the most appropriate). In §2 we define the notion of 'reversibility' for a wetting process, which gives inequalities relating contact angles viewed at macroscopic and microscopic dimensions. In particular, these may be used to derive an upper bound on the area of a solid surface that can be wetted.

Using the methods of suspension mechanics, a model of a two-dimensional random rough surface is presented in §3, and the advancing and receding contact angles on the surface are determined analytically in the limit where, macroscopically, surface-tension forces dominate over viscous forces (although on a microscopic scale these forces are comparable).

2. Static contact angles

Although the term 'static contact angle' is defined in many elementary textbooks, these definitions are often inadequate (Vennard & Street 1975). This is because the macroscopic contact angle that a fluid–fluid interface makes with a solid surface (i.e. that angle measured at a distance large compared with all microscopic lengthscales of the solid surface, but small compared with macroscopic length-scales) is, in general, a function of the history of the contact line. It depends on how the static configuration was set up as well as on the materials present. It is shown later in this section, and in detail in §3, that a cause for history-dependence is surface roughness. However, we begin by considering two situations in which the history of the contact line plays no role in determining the static contact angle. The first is when the solid surface is 'perfectly flat', i.e. flat on any lengthscale greater than the size of a molecule, as in a crystal plane, for example; and the second is when the wetting process on a rough surface is 'reversible' (in a sense to be defined later in §2.2).

2.1. *Static contact angle on a perfectly flat surface*

In the case of a perfectly flat surface the particular contact angle θ_0 is determined by insisting that the three phases (see figure 1) are in equilibrium under the action of intermolecular forces, for example, van der Waals or dispersion forces. White (1976) argued that although the fluid–fluid interface in the neighbourhood of the contact line will in general be curved, the limiting or apparent contact angle many dispersion-force lengthscales from the contact line must satisfy Young's equation

$$\sigma_{23} = \sigma_{13} + \sigma_{12} \cos\theta_0, \tag{2.1}$$

where σ_{12}, σ_{13}, σ_{23} are surface energy densities between the media denoted by the subscripts (see figure 1), also measured far from the contact line. In practice the energy densities on the solid surface are very difficult to determine, and are inferred from (2.1) using a measured θ_0. However, for our purposes we require only that θ_0 exists and is well-defined.

Note that (2.1) has real, and so physically meaningful, solutions for θ_0 if and only if

$$|\sigma_{23} - \sigma_{13}| < |\sigma_{12}|,$$

otherwise no static equilibrium is possible and spontaneous (or dynamic) wetting occurs.

2.2. *Static contact angle on a rough surface*

Throughout the rest of the paper we will use the term 'rough surface' to denote a surface that varies on a lengthscale that is large compared with the molecular scale but small compared with the macroscopic scale. On a small lengthscale the surface is taken to be a 'perfectly flat' continuum surface. In this case, it is meaningful to define a *microscopic* contact angle (i.e. the angle at which the free surface meets the tangent plane of the solid surface), which we will equate to the angle θ_0 described in §2.1. The *mean* or apparent macroscopic contact angle is, however, no longer θ_0, and generally depends upon the history of the contact-line motion (§3.7). Although the above definition of a rough surface is an idealized model of real rough surfaces, it will be seen that it exhibits all the wetting characteristics of a real rough surface.

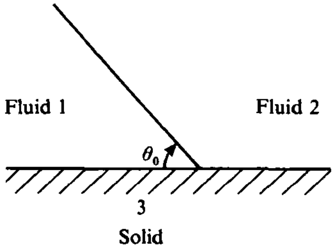

FIGURE 1. Defining diagram for static configuration.

Contact angle for reversible wetting processes

A wetting process is called 'reversible' if the net energy expended in advancing and retracting the contact line over a given macroscopic area is zero. An often-quoted result (Wenzel 1949) for this special case of reversible wetting for the static contact angle on a macroscopically homogeneous rough surface is given by

$$\cos(\theta_0+\theta_1) = \sigma \cos\theta_0, \tag{2.2}$$

where $\theta_0+\theta_1$ is the apparent contact angle (assuming it exists) measured many roughness lengthscales away from the contact line, and σ is the ratio of true area to projected area of the rough surface. A proof of this result, which will lead to some useful generalizations, will now be given. Define $\boldsymbol{n}$ and $\boldsymbol{m}$ respectively as the unit normals to the solid and free surfaces (see figure 2). The free surface satisfies the well-known Young–Laplace equation, which in terms of $\boldsymbol{m}$ may be written

$$\gamma\nabla\cdot\boldsymbol{m} = [\boldsymbol{m}\cdot\boldsymbol{\sigma}\cdot\boldsymbol{m}], \tag{2.3}$$

where γ is the surface tension of the free surface, which will generally be taken equal to unity, and $[\boldsymbol{m}\cdot\boldsymbol{\sigma}\cdot\boldsymbol{m}]$ is the normal stress jump across it. For a reversible wetting process, the normal-stress jump must be solely due to pressure forces, because energy lost by viscous dissipation can never be recovered. Now on the macroscopic lengthscale the jump in pressure will cause a curvature of the surface which will be negligibly small on the microscopic lengthscale. Hence (2.3) becomes

$$\nabla\cdot\boldsymbol{m} = 0. \tag{2.4}$$

Consider the mesoscopic volume $\mathscr{V}$ traced out by the free surface per unit width of the contact line as it wets a mesoscopic area $\mathscr{A}$ of the solid rough surface bounded above by a plane surface $\mathscr{A}_0$ (see figure 3). Note that $\mathscr{V}$ is not necessarily single-valued in real space, as the motion of the free surface need not be monotonic. However, this does not violate any of the conditions for the divergence theorem, which applied to

$$\int_{\mathscr{V}} \nabla\cdot\boldsymbol{m}\,\mathrm{d}\mathscr{V} = 0$$

implies that

$$\int_{\mathscr{A}} \boldsymbol{n}\cdot\boldsymbol{m}\,\mathrm{d}\mathscr{A} = \int_{\mathscr{A}_0} \boldsymbol{n}_0\cdot\boldsymbol{m}\,\mathrm{d}\mathscr{A}_0, \tag{2.5}$$

where $\boldsymbol{n}_0$ is the normal to $\mathscr{A}_0$. The integrals over the initial and final parts of the free surface of $\mathscr{V}$ cancel owing to homogeneity. If $\mathscr{A}_0$ is many roughness lengthscales above the solid surface, $\boldsymbol{m}$ restricted to $\mathscr{A}_0$ will be almost constant, $\boldsymbol{m}_0$, and therefore

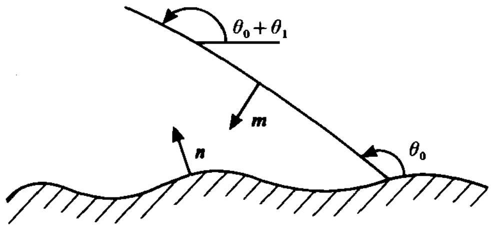

FIGURE 2. Defining diagram for contact angle on a rough surface.

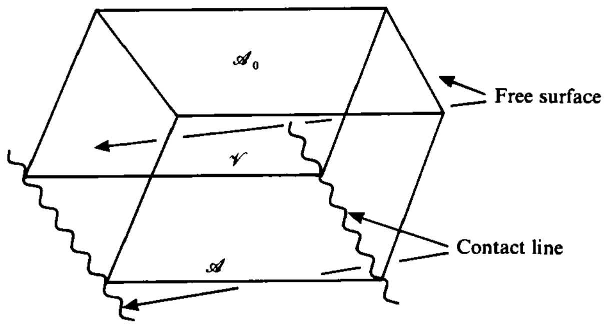

FIGURE 3. Diagram defining volume $\mathscr{V}$.

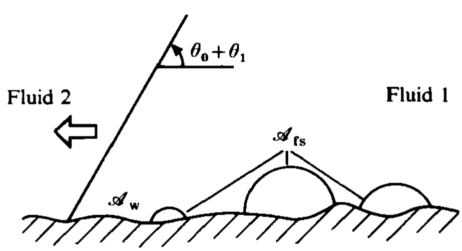

FIGURE 4. Illustration of notation when droplets are left behind.

the contact angle will also be almost constant, $\theta_0+\theta_1$. Using the boundary condition on the solid surface, $\boldsymbol{n}\cdot\boldsymbol{m} = -\cos\theta_0$, (2.5) becomes

$$\mathscr{A}\cos\theta_0 = \mathscr{A}_0\cos(\theta_0+\theta_1),$$

where $\mathscr{A}/\mathscr{A}_0 = \sigma$, thus giving the required result.

By a similar argument, we obtain a generalization which takes account of droplets left behind:

$$\cos(\theta_0+\theta_1) = \sigma_w\cos\theta_0-\sigma_{fs}, \tag{2.6}$$

where $\sigma_w = \mathscr{A}_w/\mathscr{A}_0$, $\sigma_{fs} = \mathscr{A}_{fs}/\mathscr{A}_0$, with $\mathscr{A}_w$ and $\mathscr{A}_{fs}$ defined respectively as the wetted area of $\mathscr{A}$ and the total free-surface area of the droplets left behind on $\mathscr{A}$ (see figure 4).

Although (2.2) assumes reversible wetting, it can give a useful inequality for the irreversible case. If we suppose that the driving force for contact-line motion is provided solely by surface-tension forces many roughness lengths away from the contact line, then the effect of all the dissipative processes near the contact line (e.g.

viscous dissipation) can be included in (2.6) through a dissipation per unit area term, D, giving

$$D+\cos(\theta_0+\theta_1) = \sigma_w \cos\theta_0 - \sigma_{fs}. \tag{2.7}$$

From the second law of thermodynamics, $D \geqslant 0$, which implies that

$$\cos(\theta_0+\theta_1) \leqslant \sigma_w \cos\theta_0 - \sigma_{fs}. \tag{2.8}$$

For a system where the contact angles are such that they tend to resist the motion of the contact line, i.e. $\theta_0+\theta_1$, $\theta_0 \geqslant \frac{1}{2}\pi$, (2.8) can be used to derive an upper bound on the proportion of the solid surface wetted. In this case (2.8) implies that

$$\frac{\sigma_{fs}}{\cos\theta_0}+\frac{\cos(\theta_0+\theta_1)}{\cos\theta_0} \geqslant \sigma_w. \tag{2.9}$$

Even if σ_{fs} and $\cos(\theta_0+\theta_1)$ are not known, we may use $|\cos(\theta_0+\theta_1)| \leqslant 1$ and $\sigma_{fs} \geqslant 0$ to obtain

$$\sigma_w \leqslant \frac{1}{|\cos\theta_0|}. \tag{2.10}$$

Hence if the surface is sufficiently rough that $\sigma > 1/|\cos\theta_0|$ then (2.10) implies that not all the surface can be wetted.

Calculation of the apparent static contact angle given the position of the contact line

The apparent static contact angle will depend on the history of the motion of the contact line only through its instantaneous position. In this subsection we assume that the instantaneous position is given, and we will determine it in §3. Suppose that a finite section Γ of the contact line is mesoscopically straight, and consider the portion of the free surface between Γ and a line Γ_0, in the free surface, mesoscopically parallel to Γ but many roughness lengths away (see figure 5). Then, from (2.4) we find an integral constraint corresponding to force balance on the free surface between Γ and Γ_0, namely

$$\int_\Gamma \boldsymbol{t}\,\mathrm{d}\Gamma = -\int_{\Gamma_0} \boldsymbol{t}_0\,\mathrm{d}\Gamma_0, \tag{2.11}$$

where $\boldsymbol{r}$ is a position vector and $\boldsymbol{t}$, $\boldsymbol{t}_0$ are tangents to the free surface along Γ and Γ_0 and make right-angles with them in an outward direction. Take $\hat{\boldsymbol{z}}$ as a unit vector perpendicular to Γ_0 and in the plane of the solid surface, then from (2.12) we find

$$\begin{aligned}\int_\Gamma \boldsymbol{t}\cdot\hat{\boldsymbol{z}}\,\mathrm{d}\Gamma &= -\int_{\Gamma_0} \boldsymbol{t}_0\cdot\hat{\boldsymbol{z}}\,\mathrm{d}\Gamma_0\\ &= \Gamma_0\cos(\theta_0+\theta_1).\end{aligned}$$

This may be written as

$$\cos(\theta_0+\theta_1) = \frac{\Gamma}{\Gamma_0}\overline{\boldsymbol{t}\cdot\hat{\boldsymbol{z}}}, \tag{2.12}$$

where $\overline{}$ denotes an average along Γ.

If we use (2.12) to examine a corrugated surface, we find that $(\Gamma/\Gamma_0)\overline{\boldsymbol{t}\cdot\hat{\boldsymbol{z}}}$ is independent of Γ, and equal to $\sigma\cos\theta_0$, provided that it crosses the corrugations, in agreement with (2.2). In particular, note that $(\Gamma/\Gamma_0)\,\overline{\boldsymbol{t}\cdot\hat{\boldsymbol{z}}}$ is independent of Γ on a perfectly flat surface.

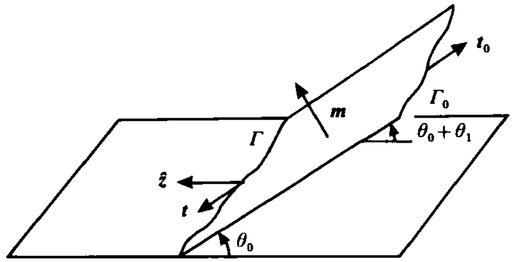

FIGURE 5. Defining diagram.

In §3 we consider surfaces that are flat except for an array of rough patches on the solid surface. Then, from (2.11), the contact angle is given by

$$\cos(\theta_0+\theta_1)-\cos\theta_0 = \frac{1}{\Gamma_0}\,\hat{z}\cdot\left\{\int_\Gamma t\,\mathrm{d}\Gamma-\int_{\Gamma'} t'\,\mathrm{d}\Gamma'\right\},$$

where Γ' is the projection of Γ onto the mean plane of the solid surface and t' is the corresponding value of t. It is clear that the only non-zero contributions to the integral are from the rough patches, and, defining n_1 as the number of rough patches along the contact line per unit length of Γ_0, we find

$$\cos(\theta_0+\theta_1)-\cos\theta_0 = -n_1\,\bar{\alpha}. \tag{2.13}$$

where $\bar{\alpha}$ is the average value of

$$-\hat{z}\cdot\left\{\int_\Gamma t\,\mathrm{d}\Gamma-\int_{\Gamma'} t'\,\mathrm{d}\Gamma'\right\}$$

per rough patch on the contact line. The quantity $\bar{\alpha}$ corresponds to a stresslet in suspension problems, as it gives the microscopic contribution to the macroscopic contact angle from each rough patch.

3. Dynamic contact angles

In this section we calculate the dynamic contact angle (i.e. contact angle for a moving contact line) explicitly for a particular class of non-reversible wetting processes. This is also crucial for understanding the history-dependence of static contact angles as the history-dependence is simply a consequence of the past dynamics. For this reason, the traditional terms 'static' and 'dynamic' are inappropriate for describing contact angles, and are better replaced by 'history-independent' (or 'reversible') and 'history-dependent' (or 'non-reversible').

The first difficulty one encounters when attempting to solve a problem with a moving contact line is that the stress has a non-integrable singularity at the contact line due to the no-slip boundary condition (Dussan V. 1979). In this section we consider the case in which surface-tension forces may be assumed to dominate viscous forces, in spite of the 'stress singularity'.

It is clear that we cannot insist on the no-slip boundary condition holding at distances of the order of molecular dimensions away from the contact line, because at these distances the fluid can no longer be considered as a continuum. So even though classically the viscous stress grows like $1/r$ at the contact line, it is clear that we must cut this off at least at a distance of molecular dimensions for a liquid (or the mean free path for a gas). This gives an upper bound for the maximum possible value of the viscous stresses at the contact line as $\mu U/\delta$, where μ is the viscosity of the more-viscous fluid, U is the normal component of velocity of the contact line along the solid surface and δ is the molecular size.

We shall assume that within δ of the contact line the only other important forces are the van der Waals forces (or 'surface-tension' forces) as was the case for the static contact angle (§2.1); note that although the notion of surface tension is not strictly meaningful this close to the contact line, it is still useful for order-of-magnitude estimates (the van der Waals forces are of the same order as surface-tension forces on a surface with curvature of order $1/\delta$). The relative importance of viscous and van der Waals forces is then given by the capillary number $\mathbb{C} = \mu U/\gamma$. The capillary number for water is usually small in practice, and is, for example, of the order of 10^{-4} for $U = 1$ cm s^{-1}, and can be made arbitrarily small for any fluid by decreasing U.

The term 'contact-angle hysteresis' has been used by most authors in the field to mean that the graph of contact angle against velocity is discontinuous at zero velocity (which is the macroscopic manifestation of a non-reversible wetting process) and *not* that the function $(\theta_0+\theta_1)(U)$ is multivalued. The phenomenon of contact-angle hysteresis has been considered by many authors, in particular Huh & Mason (1977), who analysed the spreading of a drop on several regular rough surfaces, having concentric, cross, hexagonal and radial grooves. However, the dynamic contact angles for such surfaces behave in a quite different manner from those for randomly rough surfaces, and are strong functions of the direction in which the contact line crosses the surface. Infinitesimal changes in this direction can result in large changes in the dynamic contact angle (see §3.8*e*), a feature not shared by real surfaces with microscopic roughness. Huh & Mason also attempted to calculate contact angles on random rough surfaces, but the results were in terms of height autocorrelations which were never evaluated in any specific case and this formalism is such that it can never give rise to contact-angle hysteresis. Later, Bayramli *et al.* (1981) considered theoretically the contact-line problem when a rod with macroscopic random axisymmetric grooves is vertically raised and lowered into a tank of fluid, but the contact angle is inevitably time-dependent, and only the time-averaged contact angle exhibits the characteristic hysteretic behaviour; these results of Bayramli *et al.* have been verified experimentally (Bayramli & Mason 1981).

3.1. *A model for contact-angle hysteresis on an almost-flat surface*

In order to obtain steady contact-line motion theoretically, it is necessary to consider randomly rough surfaces that are statistically homogeneous in the direction of motion. For such a calculation to be mathematically tractable, some simplifying assumption is necessary, such as that of an 'almost-flat' surface. In the past, 'almost-flat' has been taken to mean 'slowly varying' (Huh & Mason 1977), and in the analysis of Huh & Mason, the expansion parameter (i.e. typical slope) is assumed to be small compared with the ratio of microscopic lengthscales, L to macroscopic lengthscales $\mathscr{L}$, $O(L/\mathscr{L})$, which is zero in any 'thermodynamic' limit, and because of this assumption, they did not find hysteresis. We shall here take the term 'almost-flat' to mean flat except for a small areal concentration c of rough patches, and it will be shown that even for the special case of slowly varying rough patches, contact-angle hysteresis is possible! However, the characteristic surface slopes must be larger than those considered by Huh & Mason (1977), and, in fact, we suppose that we can neglect all terms $O(L/\mathscr{L})$ from the outset, i.e. all the rough patches are assumed to be small compared with macroscopic dimensions but large compared with molecules.

We will show later that the irreversibility of the wetting process for our 'almost-flat' rough surface is due to a moving contact line 'hanging on' to rough patches, thus tending to resist motion in any direction. For simplicity we shall assume that the distribution of rough patches on the solid surface is statistically homogeneous and isotropic and the rough patches themselves are all identical and similarly orientated. We also assume, for simplicity, that the microscopic contact angle $\theta_0 = \frac{1}{2}\pi$, generalizing to an arbitrary θ_0 in Appendix B.

3.2. *Structure of calculation*

In what follows, we shall calculate θ_1 to leading order in c. However, this calculation is not at all as straight-forward as its suspension-mechanical analogue, namely the determination of the particle stress to leading order. This is principally because we are not able to consider each rough patch as if alone on the contact line, because the resulting perturbation to the free surface is unbounded at infinite distances, as the fundamental solution to the linearized Young–Laplace equation is $\log(1/\rho)$, where ρ is the distance from the singularity.

Problems of this kind, where a naive formulation fails because interactions between particles have either been ignored or summed incorrectly, are often encountered in suspension mechanics. The most closely related suspension mechanical problem is probably the determination of 'the stress generated in a nondilute suspension of elongated particles by pure straining motion' (Batchelor 1971), which is also governed by the Laplace equation, so again logarithmic divergences occur in a naive formulation. However, in the rod problem, the number density of particles is known *a priori*, which is certainly not the case for the contact-line problem, as the corresponding quantity, the number density of rough patches attached to the contact line, is initially an unknown function of c.

In order to calculate the dynamic contact angle, we first analyse the behaviour of the free surface near a given rough patch ('inner problem'), where each rough patch may be considered as a 'point source of contact angle' (equation (2.14)). It is in the 'outer problem' that the 'renormalization' of the divergence of the naive one-rough-patch problem must take place.

This calculation is primarily performed to demonstrate explicitly the effect of random surface roughness on the dynamic contact angle, with particular emphasis on the microscopic mechanisms leading to contact-angle hysteresis. The problem is solved in two ways (to be described later) to illustrate how such problems may be posed more generally, as even this has caused some difficulty (Huh & Mason 1977; Bayramli *et al.* 1981) since the position of the contact line is not known *a priori*.

Kinematics of the problem

Take Cartesian coordinates such that the plane of the solid surface is coincident with the (x, z)-plane, with the z-axis in the mean direction of motion of the contact line, as shown in figure 6. Now we may define the free surface by $z = \phi(x, y)$, and (2.4), in terms of $\phi(x, y)$ becomes

$$\nabla\cdot\left\{\frac{\nabla\phi}{(1+(\nabla\phi)^2)^{\frac{1}{2}}}\right\} = 0, \tag{3.1}$$

where ∇ is the two-dimensional gradient operator.

Fortunately, we only ever have to consider the full nonlinear equation in the neighbourhood of a rough patch (attached to the contact line), and far away from any individual rough patch we may linearize (3.1), giving

$$\nabla^2\phi(x, y) = 0. \tag{3.2}$$

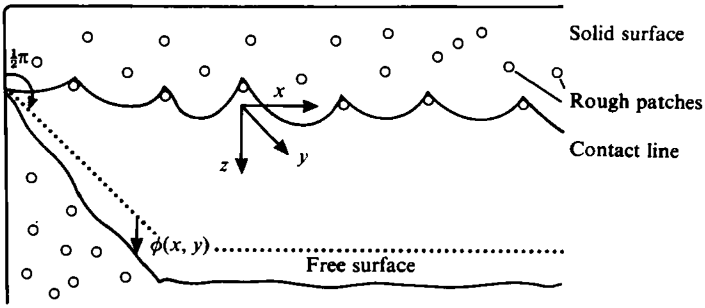

FIGURE 6. Diagram defining Cartesian axes.

Since the areal concentration of rough patches on the solid surface is assumed small, so too will be the line concentration of rough patches along the contact line (i.e. the line concentration of points where the boundary condition at the solid surface is not $\partial\phi/\partial y = 0$). In this case, it is possible to define 'inner' and 'outer' regions, the inner region being the potentially nonlinear region near a rough patch having x, y varying on a lengthscale $O(a)$ (where a is a characteristic dimension of a rough patch), and the outer (linear) region having x, y varying on the inter-rough-patch lengthscale L on the contact line. Since in the outer region each rough patch has arbitrarily small size because $a/L \rightarrow 0$, as $c \rightarrow 0$ (in fact, as will be shown later, $a/L = O(c \log c^{-1})$), its effect as regards the outer solution can be replaced by a delta-function forcing of $\partial\phi/\partial y$ at the boundary $y = 0$, i.e. $\partial\phi/\partial y \propto \delta(x-x_0)$ in the neighbourhood of a rough patch at $x = x_0$.

In order to solve the outer problem and thus determine the dynamic contact angle, we must calculate both (*a*) which rough patches are attached to the contact line, and (*b*) the strength α of the delta-function forcing representing each of these rough patches. These two calculations are coupled and depend on the past history of the contact line, with the strengths of the rough patches ultimately determined by matching with the inner solutions. We shall now discuss how contact-line history can be incorporated into the inner solution.

3.3. *The inner problem*

For simplicity we suppose that the contact-line history is such that it moves monotonically while attached to a specific rough patch. This assumption is not particularly restrictive, as we only require monotonicity of motion while the contact line moves a microscopic dimension, which we later show to be $O(a \log c^{-1})$. It is shown later that for a leading-order calculation of the dynamic contact angle, the inner solution is only important in determining α_{max}, the maximum possible strength of a rough patch.

To calculate α_{max} we must in general solve (3.1) in the neighbourhood of a rough patch, which requires a boundary condition at infinity (or more precisely, the inner limit of the outer solution). The boundary condition at infinity may be determined to leading order by solving (3.2), taking our particular rough patch at the origin and assuming it has no close neighbours (for the probability of a neighbour within $O(a)$ of the origin is zero at leading order). Thus we must solve

$$\nabla^2\phi(x, y) = 0,$$

$$\left.\frac{\partial\phi}{\partial y}\right|_{y=0} = \alpha\delta(x) + \text{a function zero near } x = 0,$$

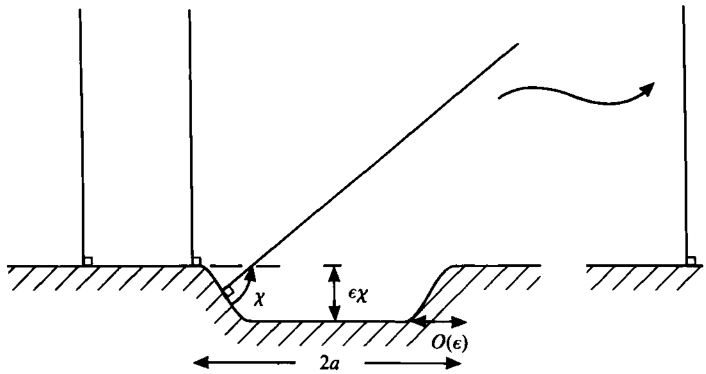

FIGURE 7. Cross-sectional view of hollow.

with $\phi(x,y)$ assumed known as $\rho/L \to \infty$, where $\rho = (x^2+y^2)^{\frac{1}{2}}$, giving

$$\phi(x,y) = \frac{\alpha}{2\pi}\log(x^2+y^2) + \text{a function regular near } x = 0. \tag{3.3}$$

Although $\phi(x,y)$ cannot be completely determined at this stage, it is known to leading order near $x = 0$, since it has a singularity there.

In general $\alpha_{\max}$ must be calculated numerically,† by advancing the contact line, solving (3.1) for various values of α with

$$\phi(x,y) \sim \frac{\alpha}{2\pi}\log(x^2+y^2) + \text{const} \quad \text{as } \rho \to \infty,$$

and increasing α until a point is reached where no solution exists. Generally this is a difficult calculation, because in the rough patch the boundary condition at the solid surface will not necessarily be at $y = 0$.

To highlight the essential physical mechanisms and yet keep the mathematics to a minimum, we shall consider a particularly simple specific example of a rough patch (shown in figure 7), a flat-bottomed circular hollow of diameter $2a$, with flat sides making an angle χ with the horizontal along the line of maximum slope, and of depth $\epsilon\chi$ ($\epsilon \ll 1$). The side region can be taken to have width $O(\epsilon)$ and to match smoothly with the flat regions, giving an overall height profile on the solid surface which is smooth. This rough patch has the convenient property that when solving the inner problem, all boundary conditions at the solid surface can be applied at $y = 0$ to leading order in ϵ/a.

We may now consider what happens as the contact line moves across the hollow, starting at the left-hand edge, as shown in figure 7. The contact line cannot move over the $O(\epsilon)$ edge region until at some point the free surface is tilted into the hollow by an amount χ, and thus is unable to increase any further. The advancing contact line therefore stops at the leading edge of the hollow and gradually wraps itself round it. When at some point (the middle, in fact) the free surface first attempts to tilt more than χ, the whole contact line peels off the hollow, and makes a catastrophic jump to a new equilibrium, which in the limit $c \to 0$ will be shown to be at least $O(a \log c^{-1})$ beyond the hollow.

It is clear then that such a rough patch has a non-zero value of $\alpha_{\max}$ for all ϵ, even

† However, see Appendix C for an analytic solution for a non-linear rough patch.

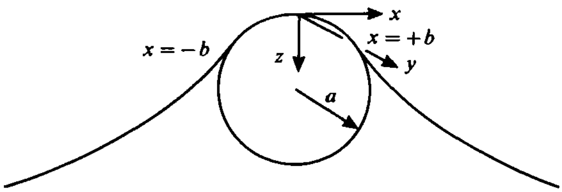

FIGURE 8. Illustration of coordinates describing hollow.

though within the hollow the area fraction of non-horizontal points can be made arbitrarily small by decreasing ϵ. Furthermore, $\alpha_{\max}$ is independent of ϵ in the limit $\epsilon \to 0$. Although it is relatively easy to calculate $\alpha_{\max}$ numerically for all values of χ, it is not particularly informative, and so we restrict calculation of $\alpha_{\max}$ to the limit of small χ.

Calculation of $\alpha_{\max}$ for small χ

In this case we may use (3.2) everywhere. Suppose that the contact line adhered to the hollow for $x \in [-b, b]$ (see figure 8), then in this range $\phi(x, 0)$ is known and equal to $-(1-x^2)^{\frac{1}{2}}$, where we have taken $a = 1$ for convenience; for consistency in using (3.2), however, we must approximate $(1-x^2)^{\frac{1}{2}}$ by $1-\frac{1}{2}x^2+O(x^4)$. We write the boundary condition for $\phi(x, y)$ at $y = 0$ as

$$\left.\frac{\partial\phi}{\partial y}\right|_{y=0} = \begin{cases} f(x) & \text{for } x \in [-b, b], \\ 0 & \text{otherwise} \end{cases}$$

where $f(x)$ is a symmetric function, unknown at this stage, satisfying

$$\alpha = \int_{-b}^{b} f(x)\,\mathrm{d}x$$

for consistency with the boundary condition at infinity. Using $(1/2\pi)\log(x^2+y^2)$ as a Green function, since it has the correct form at infinity, we find

$$\phi(x, y) = \frac{1}{2\pi}\int_{-b}^{b} f(q)\log((x-q)^2+y^2)\,\mathrm{d}q + \text{const}.$$

which gives
$$-1+\tfrac{1}{2}x^2 = \frac{1}{\pi}\int_{-b}^{b} f(q)\log|x-q|\,\mathrm{d}q + \text{const}$$

for $x \in [-b, b]$. On differentiating with respect to x, this reduces to

$$x = \frac{-1}{\pi}\int_{-b}^{b}\frac{f(q)}{q-x}\,\mathrm{d}q \quad \text{for } x \in [-b, b],$$

and is recognized as a Hilbert transform, which may be inverted to give

$$f(x) = (b^2-x^2)^{\frac{1}{2}}.$$

To calculate $\alpha_{\max}$ we observe that the contact line will first break away from the hollow at the midpoint of the rear edge (i.e. at $x = 0$), and for this we require that $f(0) = \chi$. We thus determine, in dimensional form,

$$\alpha_{\max} = \tfrac{1}{2}\pi a\chi^2(1+O(\chi^2)). \tag{3.4}$$

3.4. *Calculation of dynamic contact angle*

It is now possible to calculate the dynamic contact angle $\theta_0+\theta_1$ by solving the outer problem assuming that the contact line has been moving monotonically in the z-direction sufficiently far (in fact this will be shown to be $O(a \log c^{-1})$ for it to be possible to neglect all starting transients). In the following calculation there are two number densities which must not be confused; the first is n_1, already defined in §2 as the number of rough patches per unit macroscopic width of the contact line, which is not known *a priori*, and the second is n_2, which is defined as the area density of rough patches on the solid surface and is a given property of the solid surface equal to c/A_0. The dynamic contact angle will be determined in two ways, the first of which is by calculating the number density n_1 of rough patches on the contact line and the average strength $\bar{\alpha}$ of a rough patch on the contact line, then applying (2.14), which reduces to $\theta_1 = n_1 \bar{\alpha}$ (at leading order in c, and with $\theta_0 = \frac{1}{2}\pi$). The second mechanism supposes that $\bar{E}_0$ is the irreversible energy loss per rough patch due to non-equilibrium jumps as the contact line breaks away from them (typically radiated by capillary waves damped by viscosity). Then the irreversible work done by a contact line moving over a mesoscopic area $\mathscr{A}_0$ is $n_2 \bar{E}_0 \mathscr{A}_0$. The work done by mesoscopic surface tension forces in excess of the reversible work over the same area, as given by (2.7) with the term D set to equal $n_2 \bar{E}_0$, implies that

$$n_2 \bar{E}_0 = \sigma_w \cos\theta_0 - \sigma_{fs} - \cos(\theta_0+\theta_1). \tag{3.5}$$

This simplifies significantly in the case where $\sigma_{fs} = 0$ (i.e. no droplets are left behind), because then $\sigma_w = \sigma = 1+O(c)$. At leading order in c, since θ_1 will later be shown to be $O(c \log c^{-1})$, we may make the approximation $\sigma = 1$, in which case (3.5) reduces to

$$\theta_1 = \frac{1}{\sin\theta_0} n_2 \bar{E}_0 + O(c). \tag{3.6}$$

In fact, even in the case where $\sigma_{fs} \neq 0$, we expect, in general, almost all the droplets to be left behind on the rough patches and not to be found on the flat parts of the solid surface, where the contact line moves unimpeded. This then implies that $\sigma_{fs} = O(c)$ and $\sigma_w = 1+O(c)$, so (3.6) is still valid. However, a rigorous calculation of σ_{fs} would involve a determination of the rate at which a droplet can form, which requires consideration of van der Waals and viscous forces and is mathematically equivalent to a coalescence problem. This would introduce another non-dimensional parameter into the calculation which could be taken as the ratio of the timescale for droplet formation to a characteristic time for the contact line to move a microscopic distance. However, this additional complication will not be considered here, and we restrict ourselves to rough patches that do not induce droplet formation.

3.5. *Brief description of renormalization*

To calculate the irreversible energy loss $\bar{E}_0$, it is useful to consider $\psi = \phi(|0^B) - \phi(|0)$, where $\phi(|0^B)$ and $\phi(|0)$ are the values of ϕ just after and before a rough patch at $x = 0$ breaks for a particular realization of the rough surface. Naively, one might have thought one could have calculated the energy lost due to one rough patch leaving the contact line by considering $\phi - \phi(|0)$, but unfortunately this does not work because direct interactions between rough patches through the field equation are so weak that $\langle\phi\rangle(|0)$ does not tend to $\langle\phi\rangle$ as ρ tends to infinity, where $\langle\ \rangle$ denotes an ensemble average. However, since one rough patch breaking could (and in practice often does) cause others to break, the energy released when ϕ changes from $\phi(|\,0)$ to $\phi(|\,0^B)$ does not average to $\bar{E}_0$. A detailed analysis of the process by which a contact line moves from one quasi-equilibrium position to another is given in Appendix A.

When a particular rough patch breaks, the free surface moves forwards, increasing the load on neighbouring rough patches; but when any of them have $\alpha > \alpha_{max}$ they will also break and increase the load on their neighbours, and so on, until a state is reached where all rough patches are below their breaking points. Rough patches below breaking point behave very much like 'springs', increasing their strength to balance any increase in the driving force of the contact line; we may therefore suppose, in a self-consistent way, that in the far field they will respond linearly to small perturbations in the applied load. This far-field approximation to the response of rough patches everywhere renormalises the logarithmic divergence at infinity.

3.6. *Calculation of* ψ

Define ψ_n as ψ in the case in which n additional rough patches break before the steady state is achieved. Then to leading order $\langle\psi_n\rangle$ satisfies

$$\nabla^2\langle\psi_n\rangle = 0$$

$$\left.\frac{\partial\langle\psi_n\rangle}{\partial y}\right|_{y=0} = -\sum_{i=0}^{n}\alpha_{max}\,\delta(x-x_i)+\eta\langle\psi_n\rangle, \tag{3.7}$$

where η is the 'spring constant' for the rough patches in the far field, which is undetermined at present, and the x_i are the positions of the broken rough patches. The 'spring' is linear, to leading order in c, since many rough patches take part in the far field, and as (3.7) is itself linear, to this order of approximation ψ_n is simply the superposition of $n+1$ copies of the solution of the ψ_0 problem. Solving for $\langle\psi_0\rangle$ in terms of η, we find

$$\langle\psi_0\rangle(x,y) = \frac{\alpha_{max}}{\pi}\int_0^\infty \frac{1}{\eta+k}\,\mathrm{e}^{-ky}\cos kx\,\mathrm{d}k. \tag{3.8}$$

It is now possible to determine η by self-consistency by noting that to leading order all the motion of the free surface occurs in the discontinuous jumps due to breaking. Since we are assuming that the solid surface is statistically homogeneous, we must have

$$n_2\int_{-\infty}^{\infty}\langle\psi_0\rangle(x,0)\,\mathrm{d}x = 1, \tag{3.9}$$

i.e. on average the number of rough patches leaving the contact line exactly balances the number joining it. On substituting for $\langle\psi_0\rangle$ from (3.8), we find

$$\eta = \frac{c\alpha_{max}}{A_0\pi}\int_{-\infty}^{\infty} g(\xi)\,\mathrm{d}\xi,$$

where $g(\xi) = -\mathrm{Ci}(\xi)\cos\xi-\mathrm{si}(\xi)\sin\xi$ and Ci and si are defined in Abramowitz & Stegun (1968, p. 232). It is possible to show analytically that $\int_{-\infty}^{\infty} g(\xi)\,\mathrm{d}\xi = \pi$, a result that can also be obtained by considering directly (3.7) in the case $n = 0$, and noting that $\int_{-\infty}^{\infty}(\partial\langle\psi_0\rangle/\partial y)|_{y=0}\,\mathrm{d}x = 0$ for $\langle\psi_0\rangle$ to be well-behaved at infinity. Thus we have

$$\eta = n_2\alpha_{max}. \tag{3.10}$$

Substituting the above value of η in (3.8) thus determines $\langle\psi_0\rangle(x,y)$ completely, and as will be seen later this is all we need know about the random variable $\psi(x,y)$ for a leading-order calculation of the dynamic contact angle.

3.7. *Determination of* θ_1

We are now in a position to calculate the dynamic contact angle by either of the two methods mentioned previously.

Method 1. *Stress balance*

We need to find a relation between η and n_1, which can be obtained by considering the ψ_0 problem in the case in which it is given that there is a rough patch that does not break at $x = x_1$. In this case, we have

$$\nabla^2 \langle \psi_0 \rangle (| x_1) = 0,$$

$$\left.\frac{\partial}{\partial y} \langle \psi_0 \rangle (| x_1)\right|_{y=0} = -\alpha_{\max}\, \delta(x) + \eta \langle \psi_0 \rangle (| x_1) + \Delta\alpha_1\, \delta(x-x_1),$$

where $\Delta\alpha_1$ is the increase in strength of the rough patch at x_1, due to the breaking of the one at 0. This has solution

$$\langle \psi_0 \rangle (x | x_1) = \langle \psi_0 \rangle (x) - \frac{\Delta\alpha_1}{\alpha_{\max}} \langle \psi_0 \rangle (x-x_1).$$

Define $\psi_{\max} = \langle \psi_0 \rangle (0)$, where we have included the inner solution in $\langle \psi_0 \rangle$ to remove the infinity at the origin in the outer problem. Since the rough patch at x_1 has not broken, the contact line there will not have moved, to leading order (in fact, it would only have moved a distance $O(\alpha_{\max}/\log c^{-1})$, so $\langle \psi_0 \rangle (x_1 | x_1) = 0$, which gives

$$\langle \psi_0 \rangle (x_1) = \frac{\Delta\alpha_1}{\alpha_{\max}} \psi_{\max}.$$

Since all other rough patches on the contact line will behave in the same way as the one at x_1, η is given by

$$\eta = \frac{n_1 \Delta\alpha_1}{\langle \psi_0 \rangle (x)},$$

which implies that

$$n_1 = \frac{\eta \psi_{\max}}{\alpha_{\max}}. \tag{3.11}$$

Note that we have also shown that the assumption that η is constant (i.e. that rough patches in the far field behave as linear 'springs') is self-consistent. $\psi_{\max}$ may be determined from (3.8) by observing that

$$\langle \psi_0 \rangle (x) \sim \frac{\alpha_{\max}}{\pi} \log \frac{1}{|\eta x|}, \tag{3.12}$$

as $|\eta x| \to 0$, and that the inner solution will in general take over from this when $x = O(a)$. $\psi_{\max}$ must therefore be given, to leading order, by

$$\psi_{\max} = \frac{\alpha_{\max}}{\pi} \log \frac{1}{|\eta a|},$$

and since, for a general rough patch that will adhere to the contact line, $\alpha_{\max}$, $A_0^{\frac{1}{2}}$ and a are all of the same order of magnitude, this becomes

$$\psi_{\max} \sim \frac{\alpha_{\max}}{\pi} \log \frac{1}{c}, \tag{3.13}$$

also valid for the circular hollow if $\log \chi^{-1} \ll \log c^{-1}$.

We are now able to check our assumption that the lengthscale η^{-1} of the disturbance due to one rough patch breaking is very much greater than the typical distance n_1^{-1} between rough patches adhered to the contact line, since

$$\frac{\eta^{-1}}{n_1^{-1}} \sim \log\frac{1}{c}.$$

A large number of rough patches therefore take part in the renormalization of the ψ_0 problem, and so we would expect the contribution from each one to be small, $O(1/\log c^{-1})$. In this case, each rough patch will contribute to the renormalization of many other rough patches before it will break itself. It can be shown that even the nearest neighbour to a breaking rough patch does not, on average, have to bear a significantly greater load than many other neighbouring rough patches. This is partly due to the fact that the number density $n_1(x\,|\,0)$ tends to zero as $|x|$ tends to zero, a result that can be verified by considering two close rough patches and noting that $n_2\,(|\,0) = n_2$ (by assumption), giving the following result:

$$n_1(x\,|\,0) = n_2\,\frac{\alpha_{\max}}{\pi}\left[1-\frac{\log\dfrac{1}{|\eta x|}}{\log\dfrac{1}{\eta a}}\right] \tag{3.14}$$

for $a \ll x \ll \eta^{-1}$.

Since a large number of rough patches are responsible for renormalizing the logarithmic divergence in the ψ_0 problem, the α_i change almost continuously (in fact, small jumps of $O[\alpha_{\max}/\log c^{-1}]$) from $\alpha_i = 0$ to $\alpha_i = \alpha_{\max}$, and because (3.8) is linear in the α_i, we have that, to leading order, the average value of α_i for rough patches attached to the contact line is simply $\frac{1}{2}\alpha_{\max}$. From (2.13) we can thus determine the dynamic part of the contact angle, viz

$$\theta_1 = \tfrac{1}{2}\alpha_{\max}\,n_1 = \left[\frac{\alpha_{\max}^2}{2\pi A_0}\right] c\log\frac{1}{c}\left[1+O\left(\frac{\log\log\dfrac{1}{c}}{\log\dfrac{1}{c}},\ \frac{\log\left(\dfrac{A_0}{\alpha_{\max}a}\right)}{\log\dfrac{1}{c}}\right)\right], \tag{3.15}$$

which in the particular case of a circular hollow with $\chi \ll 1$ reduces to

$$\theta_1 = \frac{\chi^4}{8}c\log\frac{1}{c}\left[1+O\left(\chi^2,\frac{\log\log\dfrac{1}{c}}{\log\dfrac{1}{c}},\ \frac{\log\dfrac{1}{\chi^2}}{\log\dfrac{1}{c}}\right)\right]. \tag{3.16}$$

This demonstrates that the degree of contact-angle hysteresis can be a strong function of the magnitude of gradients on the solid surface, in this case depending on the fourth power, a result which might not have been anticipated. Equation (3.15) is applied to various types of rough surface in §3.8.

Method 2. Energy method

We now present the second method of calculating $\theta_0+\theta_1$, which is included because it may be of theoretical interest, as it might be a better starting point for improved theories. It is not possible to calculate the energy in the two states $\phi(|\,0)$ and $\phi(|\,0^{\mathrm{B}})$ separately without considering the full macroscopic picture. However, the difference in energy of these two states can be determined since it is perfectly well-defined in terms of the microscopic description, given by

$$E = \tfrac{1}{2}\int_0^\infty \int_{-\infty}^\infty (\nabla\phi(|0))^2 - (\nabla\phi(|0^{\mathrm{B}}))^2\,\mathrm{d}x\,\mathrm{d}y.$$

Removing $\phi(|0^{\mathrm{B}})$ in favour of ψ, we find

$$E = -\tfrac{1}{2}\int_0^\infty \int_{-\infty}^\infty (\nabla\psi)^2 + 2\nabla\psi\cdot\nabla\phi(|0)\,\mathrm{d}x\,\mathrm{d}y. \tag{3.17}$$

Contrary to its superficial appearance, this quantity is positive, and converges in spite of the occurrence of $\phi(|0)$ as ψ is sufficiently well-behaved at infinity.

It is not possible to evaluate the integral in (3.17) directly as we only know $\langle\psi\rangle$ and $\langle\phi\rangle\,(|0)$ in detail, although, as previously mentioned, many rough patches take part in each renormalization. At leading order in c, $\psi = \langle\psi\rangle$, except close to each individual rough patch, where there is a weak singularity, in the limit $c\rightarrow 0$ of strength $(\alpha_{\max}/\log c^{-1})^2$. This implies that the contributions of the singularities to the final integral may be neglected at leading order, and so it is possible to substitute $\langle\psi\rangle$ for ψ in (3.17). If we consider the case where n additional rough patches break (3.17) becomes

$$\begin{aligned}\langle E_n\rangle = -\tfrac{1}{2}\int_0^\infty \int_{-\infty}^\infty & \nabla\langle\psi_n\rangle^2\,(|x_1,\ldots,x_n) \\ & + 2\nabla\langle\psi_n\rangle\,(|x_1,\ldots,x_n)\cdot\nabla\langle\phi\rangle\,(|0,x_1,\ldots,x_n)\,\mathrm{d}x\,\mathrm{d}y.\end{aligned} \tag{3.18}$$

Since this expression is nonlinear it is not obviously true that $\langle E_0\rangle = (n+1)^{-1}\langle E_n\rangle$, although this is indeed the case, since to leading order

$$\langle\psi_n\rangle\,(|x_1,\ldots,x_n) = \sum_0^n \langle\psi_0\rangle\,(x-x_i)$$

and
$$\langle\phi\rangle\,(|0,x_1,\ldots,x_n) = \sum_0^n \langle\phi\rangle\,(x-x_i\,|\,0),$$

and it is possible to show by integrating by parts that all the cross-terms appearing in (3.18) are zero, and thus we only need to consider (3.18) for the case $n = 0$, as in method 1. This result is physically plausible: for consider the thought experiment where the rough patches break off one at a time (the other rough patches behaving as 'springs'), which on average would clearly release energy $(n+1)\langle E_0\rangle$ and achieve the same final state as the real physical processes. Since the energy released is simply a function of initial and final positions (i.e. independent of path), the real physical processes will release precisely the same amount of energy as in the above thought experiment.

From (3.18), on substituting (3.8) we find

$$\langle E_0\rangle = \frac{\alpha_{\max}^2}{2\pi}\log\frac{1}{c}\left[1 + O\left(\frac{\log\log\frac{1}{c}}{\log\frac{1}{c}}, \frac{\log(A_0/\alpha_{\max}a)}{\log\frac{1}{c}}\right)\right],$$

and combining this with (3.6), we find

$$\theta_1 = \left[\frac{\alpha_{\max}^2}{2\pi A_0}\right] c\log\frac{1}{c}\left[1 + O\left(\frac{\log\log\frac{1}{c}}{\log\frac{1}{c}}, \frac{\log(A_0/\alpha_{\max}a)}{\log\frac{1}{c}}\right)\right],$$

where we have identified E_0 with $\bar{E}_0$, which gives precisely the same result for θ_1 as in the first method. We may generalise this result to an arbitrary θ_0 using the argument presented in Appendix B, from which we find

$$\theta_1 = \sin^2\theta_0 \left[\frac{\alpha_{\max}^2}{2\pi A_0}\right] c \log\frac{1}{c} \left[1+O\left(\frac{\log\log\frac{1}{c}}{\log\frac{1}{c}}, \frac{\log(A_0/\alpha_{\max} a)}{\log\frac{1}{c}}\right)\right]. \tag{3.19}$$

It is likely that this second approach would be better suited for extending to higher-order terms in c, especially for surfaces that trap droplets of the receding fluid. It should be emphasized, however, that any such calculation would be extremely difficult and the inner problem would have to be solved numerically.

3.8. *Types of rough surface*

We are now in a position to make some statements about the sorts of roughness that contribute most to contact-angle hysteresis, making use of the analysis of earlier parts of this section. A generalization to an arbitrary θ_0 is described in Appendix B.

(*a*) *Scratched surface*

Consider an otherwise perfectly flat surface with thin scratches of length $2l$ and constant radius of curvature a (see figure 9), and, for simplicity, suppose that the slope into the scratch is again a constant $\chi \ll 1$. As the contact line approaches a particular scratch, either the relative orientation is such that the contact line first meets one of the scratch ends, in which case $\alpha_{\max}$ will be at most of the same order as the radius of curvature at the end, and so may be taken to be zero for a thin scratch, or the scratch curves away and so the contact line will adhere to it (see figure 9). If the contact line is able to run over the middle of the scratch before it has reached the ends, the condition for breaking is the same as for the circular hollow already considered in §3.3, so that

$$\alpha_{\max} = \frac{\pi a \chi^2}{2\sin^4\theta_0}[1+O(\chi^2)];$$

but if the contact line makes contact with the end nearest to the point of initial contact before it has run over the middle, it will then peel off from that end, in which case $\alpha_{\max}$ is given by

$$\alpha_{\max} = \frac{\pi b^2}{2a}\left[1+O\left(\frac{b}{a}\right)^2\right],$$

where b is the distance along the scratch between the point of initial contact and the endpoint. These results can be combined to give

$$\alpha_{\max} = \begin{cases} \dfrac{\pi a\chi^2}{2\sin^4\theta_0} & \left(|q| \leqslant \dfrac{l}{a} - \dfrac{\chi}{\sin^2\theta_0}\right), \\[2ex] \dfrac{\pi(l-|q|a)^2}{2a} & \left(\dfrac{l}{a}-\dfrac{\chi}{\sin^2\theta_0} < |q| \leqslant \dfrac{l}{a}\right), \\[2ex] 0 & \left(\dfrac{l}{a} < |q|\right), \end{cases} \tag{3.20}$$

where q is the angle between the direction of motion of the contact line (considered on mesoscopic dimensions) and the inward normal to the arc at its centre (see

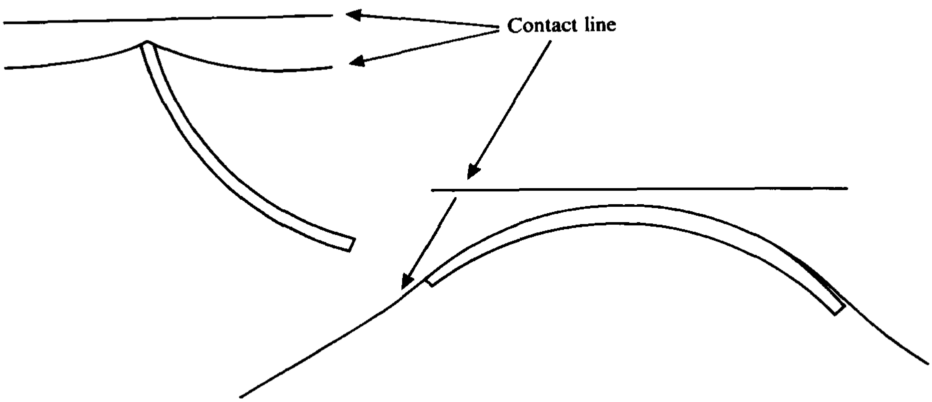

FIGURE 9. Contact line approaching a scratch at two different orientations.

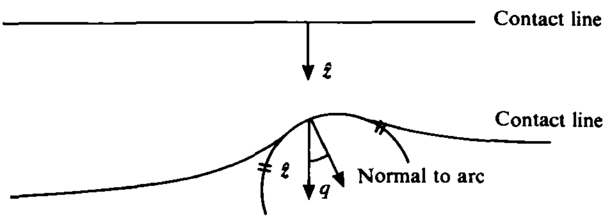

FIGURE 10. Sketch illustrating the angle q.

figure 10). From this we note that a thin straight scratch (i.e. $a = \infty$, l finite) gives a negligible contribution to contact-angle hysteresis, having at most the same order of effect as a circular hollow of radius equal to the width of the scratch. As it is not meaningful to consider the concentration of vanishingly thin scratches, we must use an alternative form of (3.15), namely

$$\theta_1 = \sin^2\theta_0 \frac{\alpha_{\max}^2}{2\pi} n_2 \left[\log \frac{1}{\alpha_{\max}^2 n_2} + O\left(\log\log \frac{1}{\alpha_{\max}^2 n_2} \right) \right], \tag{3.21}$$

or this may be cast into the old form of (3.15) by defining $c = A_0 n_2$, where $A_0 = \pi a^2$.

This shows that the degree of contact-angle hysteresis is not simply a function of the area concentration of non-horizontal points, but rather the length of rough patches to which the contact line can adhere. One consequence of this is that given an approximate surface profile (e.g. from an electron microscope), it would be very difficult to determine θ_1, as fine-scale scratches not resolved could play a crucial role.

(*b*) *Humped surface*

We have seen in the previous part of this section that very small indentations on the solid surface can have a large effect on the dynamic contact angle. In this subsection we will briefly consider how the wetting characteristic change when the surface is inverted, so that hollows are replaced by humps.

Consider the inverse of the circular hollow of §3.3, which we can think of as a low hump. When the contact line first meets the back of the hump it will have no difficulty in going up onto it, since it is downward slopes that retard the motion of a contact line, and when the contact line reaches the front of the hump where there are downward slopes of length $O(\epsilon)$ these have little effect since they behave very much like the scratches of §3.8 (a) in the case when they curve away from the direction of motion. This demonstrates that the wetting characteristics of a surface are not necessarily similar when the surface is inverted.

However, there are humps that do have a large effect, for example ones that contain hollows, or at least a ridge that curves away from the oncoming contact line, so behaving very much like a curved scratch, and humps with heights of the same order as the width (as seen from the direction of motion of the contact line), for example a hemispherical hump, which is considered in Appendix C.

(c) *Surface with anisotropic distribution of rough patches*

We have considered one way in which a rough surface can be anisotropic, namely that the rough patches themselves are anisotropic, but this can also occur through an anisotropy in the distribution of the rough patches. Although we do not intend to give a complete discussion of this here, we may give a simple illustration of how it may occur by considering a disconnected rough patch. In particular, consider a rough patch which consists of two identical rough patches of typical dimension a and distance d apart, and for simplicity suppose that $a \ll d \ll \eta^{-1}$. In this case we may define an effective $\alpha_{\max}$ for the pair, $\alpha_{\max}^{\mathrm{eff}}$, which is found to be given by

$$\alpha_{\max}^{\mathrm{eff}} = \begin{cases} 2\alpha_{\max} - \dfrac{\mathrm{d}\,|\cos q|}{\log(d/a)} & \text{for } \dfrac{\mathrm{d}\,|\cos q|}{\log(d/a)} < \alpha_{\max}, \\ \alpha_{\max} & \text{otherwise,} \end{cases} \tag{3.22}$$

where q is the angle between the direction of motion of the contact line and the line joining the two rough patches. This demonstrates how one rough patch may be shielded by another if the two are sufficiently close together, and suitably orientated so that when the contact line breaks off the first, it is almost ready to break off the second. Examining the particular cases $q = 0$ and $q = \frac{1}{2}\pi$, we find that θ_1 is respectively twice and half the value that would be obtained if the pairs of rough patches were completely unconstrained, as θ_1 is quadratic in $\alpha_{\max}^{\mathrm{eff}}$ and n_2 must be halved as the number density of pairs is half that for singletons.

(d) *Greasy surface*

Consider next a surface with patches having a different *microscopic* contact angle $\theta_0 + \theta_{\mathrm{P}}$, e.g. a surface with local contaminant, hence the term 'greasy patches'. We shall first analyse these greasy patches for the case $\theta_0 = \frac{1}{2}\pi$, generalizing later, as the dependence on θ_0 of the dynamic contact angle for these patches is quite different from that of the rough patches considered previously. For simplicity, we assume that $|\theta_{\mathrm{P}}| \ll 1$, as little additional insight would be obtained from the general case.

If $\theta_{\mathrm{P}} > 0$ the contact line will, at first, hang onto the rearmost edge of a patch, as in the case of a circular hollow, but instead of breaking suddenly, will move until it reaches a point where the length of contact line in contact with the patch is maximal, then any farther movement will cause it to break off altogether. It is possible to have discontinuous motion while in contact with the patch, as shown in figure 11. Let the maximum patch dimension perpendicular to the direction of motion be $a_{\max}$, then using the linearized form of (3.1), we have

$$\alpha_{\max} = \theta_{\mathrm{P}}\, a_{\max}.$$

Now consider $\theta_{\mathrm{P}} < 0$, which could be achieved by reversing the direction of motion, as this reverses the sense of angles; then the patches are wet more readily than the

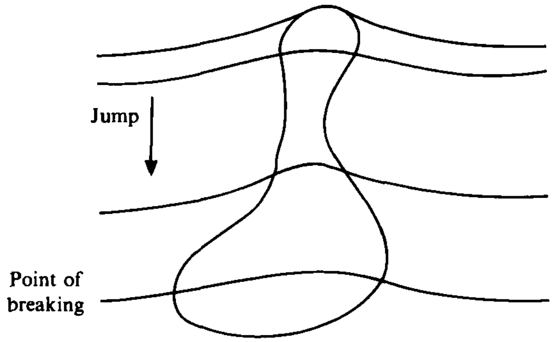

FIGURE 11. Contact line moving over a greasy patch.

uncontaminated surface, so the free surface, instead of hanging back, will be pulled forwards. However, since it cannot anticipate the patch before touching it, the time the contact line is in contact with the patch is a factor $O(1/\log c^{-1})$ shorter than for the case $\theta_P > 0$, and so to the same order $\alpha_{\max} = 0$.

To generalize our expression for $\alpha_{\max}$ to arbitrary θ_0 in this case, we simply replace θ_P by $\theta_P/\sin^2\theta_0$, giving

$$\alpha_{\max} = \begin{cases} \dfrac{\theta_P\, a_{\max}}{\sin^2\theta_0} & \text{for } \theta_P > 0, \\ 0 \quad \text{for } \theta_P < 0, \end{cases}$$

which implies that

$$\theta_1 = \frac{\theta_P^2}{\sin^2\theta_0}\left[\frac{a_{\max}^2}{2\pi A_0}\right] c \log\frac{1}{c}. \tag{3.23}$$

So in this case θ_1 is proportional to $1/\sin^2\theta_0$, as compared with $1/\sin^6\theta_0$ for the case of a circular hollow.

(*e*) *Periodic rough surface*

Consider a square array of rough patches with the contact line parallel to one of the principal axes as shown in figure 12, and take the microscopic contact angle equal to $\frac{1}{2}\pi$. We can again define inner and outer regions as in §3.2, and calculate ϕ, which is now completely deterministic. The outer problem in this case is

$$\nabla^2\phi = 0,$$

$$\left.\frac{\partial\phi}{\partial y}\right|_{y=0} = \sum_{-\infty}^{\infty} \alpha\delta(x-n),$$

where the distance between adjacent rough patches is taken as unity. The above equations may be solved by taking Fourier transforms with respect to x, giving

$$\phi(x, y) = \frac{\alpha \coth \pi y}{\cos^2\pi x + \sin^2\pi x \coth^2\pi y}.$$

If the contact line is at the point of breaking, $\alpha = \alpha_{\max}$, and (2.14) then implies that

$$\begin{aligned}\theta_1 &= n_1\alpha_{\max} \\ &= c^{\frac{1}{2}}\left[\frac{\alpha_{\max}}{A_0^{\frac{1}{2}}}\right],\end{aligned}$$

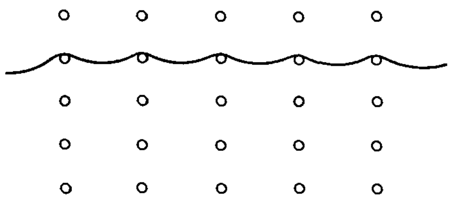

FIGURE 12. Illustration of contact line attached to a square array.

since in this case $n_1 = n_2^{\frac{1}{2}}$. After the contact line breaks off one row of rough patches, it will attach itself to the next, with α just less than $\alpha_{\max}$ by an amount $O[1/n_1 \mathscr{L}]$.

Periodic rough surfaces exhibit many characteristics that are neither shared by random surfaces nor observed in practice. For example, θ_1 is a strong function of the angle of approach to the square array, for if we turn the contact line by a small angle $q \ll c^{\frac{1}{2}} \log c^{-1}$ (see figure 13),

$$\theta_1 = \tfrac{1}{2}\left[\frac{\alpha_{\max}^2}{2\pi A_0}\right] c \log \frac{1}{c}. \tag{3.24}$$

This is derived by an argument similar to that for the random array, with unbroken rough patches behaving like 'springs'. The factor $\frac{1}{2}$ in (3.24) is due to

$$\bar{E}_0 = \frac{\alpha_{\max}^2}{2\pi} \log \frac{1}{c^{\frac{1}{2}}}$$

rather than

$$\frac{\alpha_{\max}^2}{2\pi} \log \frac{1}{c}.$$

The directions where $\theta_1 \propto c^{\frac{1}{2}}$ can be thought of as 'resonant' directions, where energy released per rough patch when a particular rough patch breaks is not related to the energy that would be released if that rough patch were suddenly removed and all others behaved as 'springs'. When the distance along the contact line between critical rough patches ($\alpha > \alpha_{\max}$) is large compared with the renormalization distance for the one-rough-patch problem, the energy released is, to leading order in c, the same as for the random case with the same value of n_1, so $\theta_1 \propto c \log c^{-1}$.

It should be noted that the strange 'resonant' behaviour of periodic rough surfaces depends on all the rough patches being perfectly placed and identical, and for this reason we would not expect it to be realised in nature for surfaces with *microscopic* roughness. It is only mentioned here because regular rough surfaces have been studied extensively by other authors, in particular Huh & Mason (1977), in whose case the surface consisted of macroscopically long grooves rather than arrays. However, the overall features would be expected to be very similar.

3.9. *Summary and conclusion*

In this section we have calculated the dynamic contact angle on a rough surface in the limit of zero C. However, this does not imply that viscous dissipation has been totally neglected, for if so we would inevitably have reproduced the results of Wenzel (1949). The moving-contact-line problem on a rough surface can be considered as a singular perturbation problem in C, so even though the mesoscopic capillary number is zero, the dissipative effect of viscosity is important. In the energy method for calculating the dynamic contact angle (§ 3.7), the net loss due to dissipative processes at the contact line is equated to the work done in excess of the reversible work by

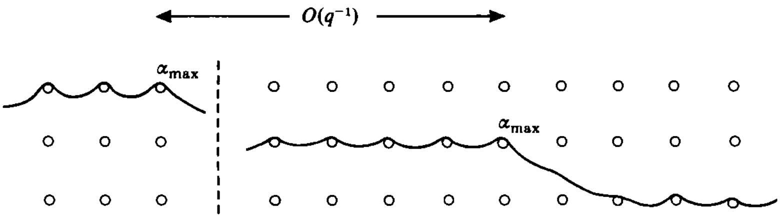

FIGURE 13. Contact line almost parallel to principal axis.

mesoscopic surface-tension forces. However, as is shown, the net effect of all the dissipative mechanisms at the contact line could be calculated by considering the energy difference between two quasisteady positions before and after the contact line makes a 'discontinuous jump'. So in effect the mesoscopic flow field does not see a *moving* contact line, but rather a stationary contact line that from time to time disappears, reappearing an instant later at a slightly advanced position. The net effect of fluid motion in the neighbourhood of the contact line during this non-equilibrium jump is accounted for in our definition of the dynamic contact angle several roughness lengths away from the contact line. The above observations have recently been used to analyse a contact line moving at non-zero $\mathbb{C}$ (Jansons 1985).

It might be thought that the random forcing of a contact line by a random array of rough patches on a solid surface is similar to the random thermal fluctuations which are important in suspension mechanics. However, one distinguishing feature is that thermal fluctuations (Brownian motion) have zero autocorrelations on the time-scales of interest, whereas a contact line encountering an area with roughness slightly greater than average for the solid surface tends to remain there for a time which is an increasing function of the strength of the fluctuation; so large fluctuations persist. This can be seen, if the rougher area is large enough for the contact angle inside it to depend on the local roughness concentration, by comparing this area with a greasy patch of §3.8 (*d*); the contact angle inside the patch is greater than outside it because of the increased roughness, implying that the contact line lingers in areas of greater roughness.

With hindsight, it is possible to see that the reason we were able to calculate the dynamic contact angle for the dilute array of rough patches, while attempts to determine dynamic contact angles failed for random slowly varying rough surfaces (i.e. surfaces with heights much less than a single characteristic wave length), is that in our analysis the history-dependence of the contact angle came in in two ways. Each rough patch has a local history corresponding to the 'inner' problem, in which we know that the contact line must approach from a particular direction and must apply a known force α_{max} to pass over the rough patch. This is then used as an input into the 'outer' problem, where we may include the statistics of the solid surface and then solve for the dynamic contact angle assuming that the contact line has moved forward sufficiently far to be in statistical equilibrium. However, a necessary assumption for this is that the chain reaction caused by one rough patch breaking always terminates with the contact line moving over an area small compared with macroscopic dimensions (see Appendix A); other details of the chain reaction have no importance to the order of approximation of this section. For a slowly varying rough surface, the behaviour of the contact line when it reaches a particular point depends crucially on the surrounding roughness, so it is not possible to incorporate the effect of the direction of motion by a local analysis. For if a slowly varying assumption were sufficient to calculate dynamic contact angles, we would expect that supposing that

Type of surface/process		θ_1
Reversible	(2.2)	$O(c)$
Random; no adherence to rough patches ($\alpha_{max} = 0$)	(3.4)	$O(c)$
Random; $\alpha_{max} \neq 0$	(3.7)	$O(c \log c^{-1})$
Periodic; 'non-resonant'	(3.8*e*)	$O(c \log c^{-1})$
Periodic; 'resonant'	(3.8*e*)	$O(c^{\frac{1}{2}})$

TABLE 1. Dependence of θ_1 on surface type, with section references.

the rough patches themselves were slowly varying would make it easier to calculate higher-order terms in concentration, which is not, in fact, the case. We conclude by presenting in table 1 a summary of the possible dependences of θ_1 on c for the rough surfaces considered in §§2 and 3.

Appendix A. The chain reaction

In this Appendix we investigate the 'chain reaction' caused by one rough patch breaking, and consider the important physical mechanisms necessary for the contact line to find a new static equilibrium. We show, in particular, that the boundary conditions at infinity before and after breaking are equal in the thermodynamic limit $a/\mathscr{L} \rightarrow 0$ with c fixed, which is an essential assumption for the analysis of §3.6. This may be achieved by first considering the chain reaction in the absence of coupling with the boundary condition at infinity for a surface with slight inhomogeneities in the direction of motion, and then secondly including these interactions by considering the stability of the contact line at macroscopic dimensions, illustrating the important physical processes by means of a particular example.

Mathematical description of the chain reaction

We divide the chain reaction up into well-defined stages by means of a simple thought experiment, defining the initial configuration, when a given rough patch is about to break as generation 0; then generation 1 is defined as the equilibrium state that would be obtained if the given rough patch were allowed to break and every other rough patch on the contact line had $\alpha_{max} = \infty$. Similarly define generation 2 as the next equilibrium state obtained by allowing every rough patch with $\alpha > \alpha_{max}$ to break, while all other rough patches on the contact line behave like 'springs' with $\alpha_{max} = \infty$, including any new rough patches that may have joined it (see §3.6). Repeating this process, we may define generations 3,4 and so on.

Now, for every rough patch breaking in generation $n-1$, a large number, $O(\log c^{-1})$, of neighbouring rough patches must increase their strength by $O(\alpha_{max}/\log c^{-1})$. So the probability distribution at leading order in c for the number of rough patches at breaking point in generation n will be given by a Poisson process that, for a system that is statistically homogeneous in the z-direction, has mean equal to the number of rough patches that were at breaking point in generation $n-1$. In addition to this, we note that at leading order in c the total excess strength $\Sigma_{\alpha_i > \alpha_{max}} \alpha_i$, in every generation is quantized (a multiple of α_{max}) provided that $\Sigma_{\alpha_i > \alpha_{max}} 1 \ll \log c^{-1}$, as for these rough patches

$$\alpha_i = \alpha_{max} \, (1 + O(\log c^{-1})^{-1}).$$

We may define the state vector of generation n as $\boldsymbol{p}^n \equiv (p_0^n, \ldots, p_i^n, \ldots)$, where p_i^n is the probability that the number of rough patches at breaking point in generation n is equal to i. Then $\boldsymbol{p}^{n+1}$ is related to $\boldsymbol{p}^n$ by the Markov process

$$\boldsymbol{p}^{n+1} = \boldsymbol{a} \cdot \boldsymbol{p}^n, \tag{A 1}$$

where a typical component a_{ij} of the matrix $\boldsymbol{a}$ is given by $a_{ij} = \mathrm{e}^{-j} j^i / i!$ $(i, j = 0, 1, 2, \ldots)$, with the convention $0^0 = 1$. The jth column of the matrix $\boldsymbol{a}$ is simply the probability distribution of a Poisson process with mean j, and (A 1) states that the actual number of rough patches above critical in generation n gives the expected number of rough patches above critical in the next generation, a consequence of statistical homogeneity.

In order to show that the chain reaction stops, we need to show that, with probability 1, in a finite number of generations we reach a state where there are no rough patches at breaking point, and so the contact line stops moving. It is possible, after a little algebra, taking initial conditions $\boldsymbol{p}^0 = (0, 1, 0, 0, \ldots)$, to derive a recurrence relation for p_0^n, namely

$$p_0^{n+1} = \mathrm{e}^{-(1-p_0^n)}, \tag{A 2}$$

a result that may be proved by mathematical induction on n. From this we deduce that $\lim_{n\to\infty} p_0^n = 1$, noting that p_0^n is an increasing function of n and that $p_0^n = 1$ is a fixed point of (A 2).

Although in any particular realization the contact line will stop after moving a finite distance, the *average* distance moved as calculated from (A 1) is infinite. This is to be expected, since the position of the contact line is ultimately determined by the *macroscopic* physics, e.g. a circular drop spreading on a plane surface, due to a volume source at its centre, continually adjusts itself to accommodate an increasing volume of fluid. This could not be so if the motion on the microscopic scale were not coupled in some way to that on the macroscopic scale.

To understand this coupling physically, consider the situation after a small amount of volume has been added to the drop. This slightly changes the boundary condition at infinity for the microscopic problem, and could result in at least one rough patch breaking. Often the contact line will stop after moving over a microscopic area, but occasionally a chain reaction will occur, which, if unchecked, would result in the contact line moving over a macroscopic area. However, in practice for such a chain reaction, the boundary condition at infinity would be relaxed sufficiently for all the rough patches to be below breaking point by the contact line moving over a mesoscopic area, and it is this coupling between the microscopic and macroscopic physics which must be included for a detailed understanding of the stopping mechanism. To include this coupling with the boundary condition at infinity in (A 1) it is helpful to consider a system that is slightly inhomogeneous in the direction of motion, for this gives the possibility of an infinite chain reaction.

Systems inhomogeneous in the z-direction

Consider a system in which the roughness varies on a lengthscale $\mathscr{L}_z$ in the z-direction, and assume that $\psi_{\max}/\mathscr{L}_z \ll 1$. For such a system we may calculate the dynamic contact angle by making a quasihomogeneous approximation, as the inhomogeneities can be ignored in the ψ_0 problem. Since the roughness is characterized by $(\alpha_{\max}^2/A_0)\, c \log c^{-1}$, we can consider a rough surface in which c only is a function of z; this significantly simplifies the chain-reaction problem as the excess strength at each generation is still quantized as before. In spite of the last assumption, the resulting macroscopic physics is the same as in the general case. If we temporarily ignore the coupling between microscopic and macroscopic, only considering the statistical inhomogeneities associated with the roughness on the solid surface, it is possible to show that the transition matrix $\boldsymbol{a}$ for the chain reaction is given by

$$a_{ij} = \frac{\mathrm{e}^{-\lambda j}\,(\lambda j)^i}{i!}, \tag{A 3}$$

where
$$\lambda = 1 - \tfrac{1}{2}\frac{\partial n_2}{\partial z}\int_{-\infty}^{\infty} \langle\psi_0\rangle^2\,(|0)\,\mathrm{d}x,$$

which holds for $\lambda \approx 1$. We may interpret λ as the expected number of rough patches to reach breaking point in generation n per rough patch in generation $n-1$.

Equation (A 2) becomes

$$p_0^{n+1} = \mathrm{e}^{-\lambda(1-p_0^n)}, \tag{A 4}$$

from which we can show that the expected number of rough patches to break in a single chain reaction is equal to

$$\begin{array}{cl} -\lambda_1^{-1} & \text{for } \lambda_1 < 0, \\ \infty & \text{otherwise,} \end{array}$$

where $\lambda_1 = \lambda - 1$, and the probability $q(\lambda)$ of an infinite chain reaction is given by

$$q(\lambda) = \begin{cases} 0 & \text{for } \lambda_1 < 0, \\ 2\lambda_1 & \text{otherwise.} \end{cases} \tag{A 5}$$

To include the coupling between microscopic and macroscopic, we note that on the microscopic scale this coupling will manifest itself by slightly changing the expected number of rough patches joining the contact line, and so, to leading order, will affect only the chain reaction and not the ψ_0 problem. Since to leading order, the amount the boundary condition at infinity is changed is proportional to the volume of fluid displaced (or the area of solid surface covered) due to discontinuous jumps of the contact line, the coupling may be included in λ.

Consider again a circular drop with a source at its centre and suppose that the contact angle is approximately $\frac{1}{2}\pi$. Since we have assumed that $C \ll 1$, the timescale for volume change is very much greater than that for microscopic adjustments. We may calculate the contribution to λ from the macroscopic constraints by another thought experiment. Consider the effect of a radial roughness down-gradient on the stability of the drop. If the gradient is steep enough the resulting advancing dynamic contact angle will decrease sufficiently fast for the drop to be unstable to small radially symmetric disturbances. The critical gradient of the dynamic contact angle is given by

$$\left.\frac{\partial \theta}{\partial z}\right|_{\text{crit}} = -\left[\frac{3\mathscr{V}}{16\pi}\right]^{-\frac{1}{3}}, \tag{A 6}$$

where $\mathscr{V}$ is the volume of the drop, which is derived by considering the drop in the thermodynamic limit $a/\mathscr{V}^{\frac{1}{3}} \rightarrow 0$ with c fixed. Since to leading order the two contributions to λ_1 are independent, we can use (A 6) to calculate the contribution to λ_1 from the macroscopic constraints, because at the critical point in our thought experiment, λ_1 must be exactly zero, as this describes the point of marginal stability in the microscopic description. We thus find that for a general concentration gradient, λ_1 is given by

$$\lambda_1 = \frac{\alpha_{\max}}{\pi^2}\int_{-\infty}^{\infty} g^2(\xi)\,\mathrm{d}\xi\left[\frac{\partial \log c^{-1}}{\partial z} - \left.\frac{\partial \log c^{-1}}{\partial z}\right|_{\mathrm{crit}}\right], \tag{A 7}$$

and from (A 6) we deduce that in our particular example

$$\left.\frac{\partial \log c^{-1}}{\partial z}\right|_{\mathrm{crit}} = \frac{1}{\theta_1}\left[\frac{3\mathscr{V}}{16\pi}\right]^{-\frac{1}{3}}. \tag{A 8}$$

We can now return to the case of a homogeneous rough surface, still retaining the term including the microscopic effect of the macroscopic constraints by setting $\partial \log c^{-1}/\partial z$ equal to zero in (A 7). From this we can deduce that the expected number of rough patches to break in one chain reaction is

$$O\left[\frac{c \log c^{-1}\,\mathscr{V}^{\frac{1}{3}}}{\alpha_{\max}}\right],$$

which we can immediately see to be of the same order as the number of rough patches on the whole contact line, although the area covered in a typical chain reaction is of mesoscopic proportions, as it is $O(a\mathscr{V}^{\frac{1}{3}} \log c^{-1})$.

It should be pointed out, however, that in the above argument we have neglected inhomogeneities along the contact line. These certainly play an important role, as it is these inhomogeneities that ensure that the drop in our thought experiment remains approximately circular, although they are not important in explaining the gross features of the chain reaction. We have therefore shown that we were correct in assuming that the chain reaction stops and that the ψ_0 problem was indeed appropriate for calculating the dynamic contact angle.

It is interesting to notice that $\lambda_1 = 0$ resembles a 'phase-transition' point, with the probability of an infinite chain reaction (one of macroscopic extent) being zero for $\lambda_1 < 0$, and increasing linearly for $\lambda_1 > 0$. The macroscopic manifestation of this is that for a system with $\lambda_1 < 0$ the contact-line motion is driven from infinity and it is possible to have motion for arbitrarily small C, as the discontinuous jumps made by the contact line are only microscopic; but for a system with $\lambda_1 > 0$ there is a finite probability of a chain reaction leading to a macroscopic movement of the contact line. So in the thermodynamic limit the contact-line position is unstable and the resulting movement of the contact line is dominated by the viscous singularity rather than the radiation of capillary waves.

The chain reactions described in this Appendix give a semiquantitative description of the well-known phenomenon of stick–slip (Dussan V. 1979) and explain why the observed jumps in contact line motion for contact lines moving with small C are very much greater than a typical roughness dimension.

Appendix B. Dynamic contact angle for a general θ_0

Consider the generalization of the expressions for the dynamic contact angle obtained previously for $\theta_0 = \frac{1}{2}\pi$ to an arbitrary θ_0, in the case where we may use the linearized form of (3.1) everywhere. To generalize to arbitrary θ_0 in the case where the inner problem is nonlinear, we must resolve the inner problem, calculating $\alpha_{\max}$ for the appropriate value of θ_0; however, the subsequent argument follows through just as in the fully linearized case.

Writing $\phi = \phi_0 + \phi_1$, where $\phi_0 = \tan(\theta_0 - \frac{1}{2}\pi)\, y$, which would be the value of ϕ for a completely flat surface, (3.1) reduces to

$$\nabla^2 \phi = 0$$

to leading order in ϕ_1.

The inner problem to calculate the value of $\alpha_{\max}$ is essentially the same as before; the only difference is in the boundary condition for ϕ_1 at $y = 0$.

Consider again the circular hollow of §3.3 (assuming $\chi \ll 1$ for linearity). The condition for breaking for $\theta_0 = \frac{1}{2}\pi$, and indeed in general, is that at the back of the rough patch the free surface makes an angle χ with its unperturbed value and so allows the contact line to run over the rough patch. This gives the new condition for breaking, that at the midpoint of the back of the hollow

$$\left.\frac{\partial \phi}{\partial y}\right|_{y=0} = \tan(\theta_0 + \chi - \tfrac{1}{2}\pi),$$

which in terms of ϕ_1 is

$$\left.\frac{\partial \phi_1}{\partial y}\right|_{y=0} = \frac{\chi}{\sin^2 \theta_0}. \tag{B 1}$$

Note that this analysis is not uniformly valid in θ_0, and actually breaks down when $\theta_0 = 0, \pi$. These particular limits are extremely difficult to deal with analytically, as we cannot apply boundary conditions at the solid surface at $y = 0$. Thus $\chi/\sin^2\theta_0$ replaces χ in the analysis of §3.3, and hence the expression for $\alpha_{\max}$ becomes $\alpha_{\max} = \pi a \chi^2/2 \sin^4 \theta_0$.

The intricate calculation of $\partial\phi_1/\partial y$ as $y \rightarrow 0$, including the renormalization and chain-reaction problems, is unchanged, as the field equation is the same and each rough patch is still described to leading order in terms of the single parameter $\alpha_{\max}$, which implies that

$$\theta_1 = \sin^2\theta_0 \left[\frac{\alpha_{\max}^2}{2\pi A_0}\right] c \log\frac{1}{c}. \tag{B 2}$$

Evaluating this for the circular hollow, we find

$$\theta_1 = \frac{\chi^4}{8 \sin^6 \theta_0} c \log \frac{1}{c}. \tag{B 3}$$

Appendix C. An analytic solution for a nonlinear rough patch

Consider a solid surface with a random array of hemispherical humps of radius a, and a microscopic contact angle equal to $\frac{1}{2}\pi$. If we examine the sequence of events as the contact line moves across a particular hump, we find that, on touching it, the contact line will immediately jump to its equator to leading order in c, and then will gradually move round towards the back, increasing α until it is maximized (see figure 14).

Since $\theta_0 = \frac{1}{2}\pi$, the free surface is axisymmetric, with axis in the direction of $\hat{\boldsymbol{z}}$, in the neighbourhood of any particular hump, and so in effect we need to calculate the maximum force that the free surface can exert on a sphere. If q is the angle between $\hat{\boldsymbol{z}}$ and the radius of the sphere to the contact line (see figure 14), the force exerted by the free surface is given by

$$F(q) = 2\pi a \sin q \cos q.$$

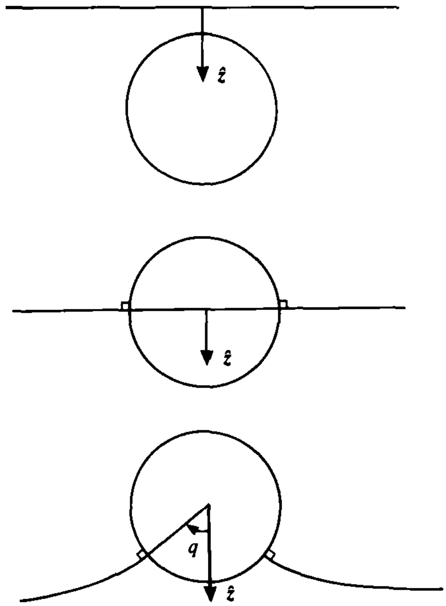

FIGURE 14. Plan view showing sequence of contact-line positions as it moves over the hump.

This force is maximized at $q = \frac{1}{4}\pi$, so $F_{\max} = a\pi$. Since $\alpha_{\max}$ is simply the force on a hemisphere, we find

$$\alpha_{\max} = \tfrac{1}{2}\pi a, \tag{C 1}$$

which on substitution into (3.15) gives

$$\theta_1 = \tfrac{1}{8}\, c \log\frac{1}{c}\left[1 + O\left(\frac{\log\log c^{-1}}{\log c^{-1}}\right)\right]. \tag{C 2}$$

Clearly this analysis may be extended to all humps that are axisymmetric about $\hat{z}$.

REFERENCES

ABRAMOWITZ, M. & STEGUN, I. A. 1968 *Handbook of Mathematical Functions*. Dover.

BATCHELOR, G. K. 1971 The stress generated in a non-dilute suspension of elongated particles by pure straining motion. *J. Fluid Mech.* **46**, 813.

BAYRAMLI, E. & MASON, S. G. 1981 Tensiometric studies on wetting. II. Some effects of surface roughness (experimental). *Can. J. Chem.* **59**, 1962.

BAYRAMLI, E., VAN DE VEN, T. G. M. & MASON, S. G. 1981 Tensiometric studies on wetting. I. Some effects of surface roughness (theoretical). *Can. J. Chem.* **59**, 1954.

COX, R. G. 1983 The spreading of a liquid on a rough solid surface. *J. Fluid Mech.* **131**, 1.

DUSSAN, V., E. B. 1979 On the spreading of liquids on solid surfaces: static and dynamic contact lines. *Ann. Rev. Fluid Mech.* **11**, 371.

HUH, C. & MASON, S. G. 1977 Effects of surface roughness on wetting (theoretical). *J. Coll. Sci.* **60**, 11.

JANSONS, K. M. 1985 Moving contact lines at non-zero capillary number. Submitted to *J. Fluid Mech.*

VENNARD, J. K. & STREET, R. L. 1975 *Elementary Fluid Mechanics*. Wiley.

WENZEL, R. N. 1949 *J. Phys. Colloid. Chem.* **53**, 1466.

WHITE, L. R. 1976 On deviations from Young's equation. *J. Chem. Soc. Faraday Trans.* I **73**, 390.